

Detection and characterization of in vitro payload-containing catabolites of non-cleavable ADCs by high-resolution mass spectrometry and multiple data-mining tools

Tingting Cai[#], Liqi Shi[#], Huihui Guo, Ruixing Li, Weiqun Cao, Liang Shen, Mingshe Zhu*, Yi Tao*.

DMPK Service Department, WuXi AppTec, Nanjing, Jiangsu, China (T.C.)

DMPK Service Department, WuXi AppTec, Shanghai, China (L.S., R.L., W.C., L.S., Y.T.)

Hangzhou DAC Biotechnology Co. Ltd., Hangzhou, China (H.G.)

MassDefect Technologies, Princeton, NJ, USA (M.Z.)

These two authors contributed equally to this manuscript.

Suggested running head:

Identification of payload-containing catabolites of ADCs

***Corresponding author:**

Yi Tao

DMPK Service Department,

288 Fute Zhong Road, Waigaoqiao Free Trade Zone, Shanghai 200131, China.

Phone: 86(21)3870-9334.

Email: tao_yi@wuxiapptec.com;

Minshe Zhu

MassDefect Technologies

Princeton, NJ 08540

Phone: 609 694-3946

E-mail: mingzhu@zoryaconsulting.com

Number of text pages:

Number of tables: 2

Number of figures: 5

Number of references: 47

Abstract word count: 249

Introduction word count: 747

Discussion word count: 1499

Nonstandard abbreviations:

ADC, antibody drug conjugates

ACN, acetonitrile

CID, collision induced dissociation

DDA, data dependent acquisition

EIC, extracted ion chromatographic analysis

HLL, human liver lysosomes

LC-HRMS, liquid chromatography coupled with high-resolution mass spectrometry

MMAF, Monomethyl auristatin F

PCC, payload-containing catabolite

PATBS, precision and through background subtraction

PIF, product ion filtering

TCEP, tris (2-carboxyethyl) phosphine

T-DM1, ado-trastuzuma emtansine, Kadcyla

UV, ultraviolet

ABSTRACT

The formation and accumulation of payload-containing catabolites (PCCs) from a non-cleavable ADC in targeted and normal tissues are directly associated with the therapeutic effect and toxicity of the ADC, respectively. Understanding the PPC formation is important for supporting the payload design and facilitating preclinical evaluation of ADCs. However, detection and identification of PCCs of a non-cleavable ADC are challenging due to their low concentrations and unknown structures. The main objective of this study was to develop and apply a generic LC-HRMS method for profiling PCCs *in vitro*. Non-cleavable ADCs, T-DM1 and ADC-1, were incubated in liver lysosomes, liver S9 and/or cancer cells followed by data acquisition using liquid chromatography-high resolution mass spectrometry (LC-HRMS). Profiling PCCs mainly relied on processing LC-HRMS datasets using untargeted background subtraction processing (PATBS) and targeted product ion filtering (PIF). As a result, 12 PCCs of T-DM1 were detected and structurally characterized in human liver lysosomal incubation, a majority of which consisted of MCC-DM1 and a few amino acids. Additionally, the incubation of ADC-1 in human, rat and money liver S9 and cancer cells generated one major and three very minor PCCs, verifying the payload design. The results demonstrate that PATBS enabled the comprehensive profiling of PCCs regardless of their molecular weighs, charge states, and fragmentations. As a complementary tool, PIF detected specific PCCs with superior sensitivity. The combination of the *in vitro* metabolism systems and the LC-HRMS method is a useful approach to profiling *in vitro* PCCs of non-cleavable ADCs in support of drug discovery programs.

SIGNIFICANCE STATEMENT

Profiling in vitro payload-containing catabolites (PCCs) of a non-cleavable ADC is important for optimization of the payload design and preclinical evaluation of ADC. However, currently used analytical approaches often fail to quickly provide reliable PCC profiling results. The work introduces a new LC-HRMS method for comprehensive and rapid detection and characterization of PCCs released from a non-cleavable ADC in liver lysosomes and S9 incubations.

Introduction

Antibody drug conjugate (ADC) is a relatively new biotherapeutic modality, composed with a monoclonal antibody, linker, and payload (or toxin) (Khongorzul et al., 2020; Mukherjee et al. 2019). The monoclonal antibody targets the antigen expressed on cancer cells and delivers the toxic payload into the cells. The high specificity of ADCs makes it a fast-growing and important drug platform in the treatment of various diseases (Peters and Brown, 2015; Chau et al., 2019; Nobre et al., 2019). ADC linkers include cleavable and non-cleavable types, depending on how they are cleaved when releasing the payload or payload containing catabolites (PCCs) (Kommineni et al., 2020; Pander et al., 2022). Cleavable ADCs release the payloads or a payload derivative in a predicted manner under a certain intracellular environment, such as low pH, protease, high GSH concentration etc. (Bargh et al., 2019; Anami et al., 2018; Bargh et al., 2021). Non-cleavable ADCs usually don't undergo specific cleavages of linkers to release the payload. Instead, they generate one or a few major unknown payload-containing catabolite(s) via protein hydrolysis of the antibody moiety (García-Alonso et al., 2018). The release of the payload or major PCCs in targeted cancer cells plays the dominant role in the therapeutic effect of the ADC (Zhang et al., 2018). Besides, the toxicity of an ADC is directly associated with the release or accumulation of the payload or PCCs in untargeted normal cells or tissues. In early discovery, it is necessary to identify the major pharmacologically active payload-containing catabolite(s) of a non-cleavable ADC *in vitro*. The information is also required to develop a bioanalytical method for evaluating exposure of the toxic PCC in animals and human (Khera and Thurber, 2018) and to study its metabolism and *in vitro* DDI potentials as parts of preclinical evaluation of the ADC (Kraynov et al., 2016; Han and Zhao, 2014; Widdison et al., 2015; Hinrichs and Dixit, 2015).

For characterization and quantification of ADCs, various bioanalysis methods have been developed (Wei et al., 2017; Zhu et al., 2020), such as immuno-capture to enrich ADCs followed by LC-MS analysis, ligand binding assay for analyzing total antibody or drug conjugated species, and intact protein characterization by LC-HRMS. However, there are a very limited publications of applying analytical technologies for profiling and identifying *in vitro* or *in vivo* PCCs of ADCs in the literatures (Saad et al., 2015; Shadid et al., 2017). Usually, concentrations of PCCs of an ADC are much lower than metabolites of small molecular drugs. Unpredictable molecular weights, mass defect values and fragmentation of payload-containing catabolites released from a

non-cleavable ADC further increase the complication of the analysis (Rangan et al., 2015; Su and Zhang, 2021). Thus, detection and structural characterization of PCCs of non-cleavable ADCs as well as their metabolites *in vitro* and *in vivo* still pose a major analytical challenge. LC-UV is used for detection and quantitative estimation of payload-containing components in biological samples, which requires high concentrations of analytes (Wei et al., 2017). LC-HRMS based full scan MS analysis and triple quadrupole LC-MS based neutral-loss scan have been employed in detection of PCCs of ADCs in lysosomal incubations (Bessire and Subramanyam, 2020), which are only suited for targeted analysis of known or predictable payload or PCCs. Commonly used LC-HRMS data processing tools for metabolite profiling of a small molecular drugs, such as mass defect filter and targeted extracted ion chromatographic analysis, are not effective in finding PCCs. So far, the most effective way to profile and characterize PCCs of ADCs is to use an ADC with radiolabeled payload or linker (Bolleddula et al., 2020; Erickson et al., 2012; Baron et al., 2015). However, the preparation of such a radiolabeled ADC is time-consuming and costly, and not well suited in drug discovery. Additionally, LC-radiodetection may not have sufficient sensitivity to detect low levels of radiolabeled PPCs.

The main objective of this study was to develop and apply a generic and effective LC-HRMS method for comprehensive detection and characterization of *in vitro* PPCs of a non-cleavable ADC using both untargeted background subtraction processing (PATBS) and targeted product ion filtering (PIF). The effectiveness of the LC-HRMS based method was first evaluating by analyzing PCCs generated in incubation of a well-known non-cleavable ADC (T-DM1) in human liver lysosomes. Its major payload-containing catabolites have been fully characterized (Shen et al., 2012). The method was further applied to profiling PCCs formed in incubations of ADC-1, a non-cleavable ADC, with human liver S9 and a cancer cell line. Results from these studies demonstrate that PATBS enabled the comprehensive detection and characterization of PCCs regardless of their molecular weighs, charge states, and fragmentations. As a complementary tool, PIF detected specific PCCs with superior sensitivity. The combination of the *in vitro* metabolism systems and the LC-HRMS method can serve for fast, sensitive, and selective profiling of *in vitro* PCCs of non-cleavable ADCs in support of drug discovery programs.

Materials and Methods

Chemicals and reagents.

T-DM1 (ado-trastuzuma emtansine, Kadcyra) and its antibody (trastuzumab) were purchased from BioChemPartner (Shanghai). ADC-1 and its corresponding antibody formulation were provided by DAC Biotech. ADC-1 is a non-cleavable ADC with monomethyl auristatin F (MMAF) as its payload component. Pooled rat, monkey, human liver S9 and human liver lysosomes were obtained from Sekisui XenoTech, LLC (Kansas, KS). Sodium acetate and tris (2-carboxyethyl) phosphine (TCEP) were from Sigma-Aldrich (Burlington, MA). Acetonitrile (ACN) was from Merck (Kenilworth, NJ). Ultrapure water was freshly prepared with Millipore purification system (Massachusetts, USA).

Incubation of TDM1 in human liver lysosomes

T-DM1 (0.5 mg/mL) was incubated in human liver lysosomes (HLL) (0.2 mg/mL) in with sodium acetate (50 mM, pH 5.0) and TCEP (2 mM) for 48 hours (Rangan et al., 2015). A negative control antibody (trastuzumab) was also incubated under the same conditions. At the end of each time point, incubation samples (400 μ L) were quenched by chilled ACN (800 μ L), then centrifuged at 13000 g for 15 min. Supernatants were dried under a gentle stream of N₂ gas. The residues were reconstituted in 200 μ L of 30 % ACN in water for LC-HRMS analysis.

Incubation of ADC-1 in rat, monkey, and human liver S9

The ADC-1 (1 mg/mL) was incubated with human liver S9 in 50 mM sodium acetate (pH 5.0) for 0, 24 and 48 hours. The control antibody of ADC-1 was also incubated under the same conditions. Incubation samples (400 μ L) at the end of each incubation time were quenched by chilled ACN (800 μ L), then centrifuged at 13000 g for 15 min. Supernatants were dried under N₂ flow and reconstituted with a mixture of ACN and water (1:9, 200 μ L) for LC-HRMS analysis.

Incubation of ADC-1 in cancer cells

Human breast cancer cells MDA-MB-468 cells were from National Collection of Authenticated Cell Cultures (<https://www.cellbank.org.cn/>) and incubated with Leibovitz's L-15 complete incubation medium. The stock solution of ADC-1 and its control antibody were

diluted with incubation medium to obtain a final concentration of 20 µg/mL. MDA-MB-468 cells were resuscitated using incubation medium at 37 °C with saturated humidity in the incubators. The cells were expanded and continuously cultured until the logarithmic growth phase, then digested with 0.25% trypsin. The cells were transferred into a 75T cell culture flask with 3×10^6 cells and total volume of 15 mL per flask. After the cells adhered, the culture medium was slowly aspirated. 15 mL of the incubation medium with spiked ADC I or antibody was added and mixed gently to initiate the incubation for 0, 24, 48 h. At each time point, the culture medium was slowly removed. The cells were digested with 0.25 % trypsin, resuspended in 10 mL of incubation medium, and then centrifuged at 1000 rpm for 5 min. The cell pellet was collected and washed with 10 mL PBS buffer, following with centrifugation at 1000 rpm for 5 min. The wash step was repeated for three times, then the cells were resuspended with 500 µL of water and extracted with 1.5 mL of ACN. The supernatant was centrifuged at 10000 rpm for 10 min. The extracts were dried under N₂ flow and reconstituted with a mixture of ACN and water (1:9, 200 µL) for LC-HRMS analysis.

LC-HRMS analysis of incubation samples

The T-DM1 and its control antibody incubation samples were analyzed by an Acquity UPLC system (Waters Corp, New Milford, MA) interfaced to a Q Exactive plus mass spectrometer (Thermo Fisher, San Jose, CA). Mobile phase A was H₂O with 0.1% formic acid, and the mobile phase B was ACN with 0.1% formic acid. Individual processed samples (20 µL) were injected on a Waters HSS T3 column (2.1 ×100 mm, 1.8 µm) at a flow rate of 0.5 mL/min. The oven temperature for column was set at 40 °C. The gradient was started at 5% B and held for 1 min, increased to 60% B at 14 min, and reached 95% B at 16 min and held for 2 min, then back to 5% B at 18.1 min. The total run time was 20 min. A full MS scan (*m/z* 150-2000) was acquired with the spray voltage of 3.5 kV in positive ion mode. The capillary temperature was 375 °C and the probe was heated under 350 °C.

The incubation samples of ADC-1 and its control antibody were analyzed by a Shimadzu UFLC 20A system (Shimadzu, Japan) coupled with a Q Exactive mass spectrometer (Thermo Fisher, San Jose, CA). Mobile phase A was H₂O: ACN (95:5) with 0.1% formic acid and 2 mM ammonium formate, and the mobile phase B was ACN: H₂O (95:5) with 0.1% formic acid and 2 mM ammonium formate. Individual processed samples (20 µL) were injected and separated on a

Waters HSS T3 column (3.0×100 mm, 2.5 μm) at a flow rate of 0.3 mL/min and oven temperature of 30 °C. For the liver S9 samples, the gradient was started at 0% B and held for 3 min, increased to 5% B at 5 min, and reached 25% B at 12 min, then 50% B at 25 min, and 95% B at 35 min, holding until 40 min, then back to 0% B at 40.1 min. The column was re-equilibrated for 7 min for the next injection. For the tumor cell incubation samples, the gradient was started at 5% B and held for 5 min, increased to 50% B at 50 min, and reached 95% B at 51 min and held until 53 min, then back to 5% B at 53.1 min. The column was re-equilibrated for 5 min for the next injection. The spray voltage of 3.5 kV in positive ion mode. The capillary temperature was 350 °C and the probe was heated under 300 °C.

LC-HRMS data processing

The acquired accurate mass LC-MS dataset of the testing ADC was processed using an in-house developed precision and through background subtraction (PATBS) software (Zhang and Yang, 2008; Zhang et al., 2008) for untargeted detection of payload-containing catabolites. The detailed working mechanism and algorithm of PATBS have been previously described (Zhang et al., 2008). LC-MS datasets of respected control antibody incubation sample as well as a preincubation sample of the ADC incubation sample were used as controls background in the data processing. The mass tolerance window was set at ± 10 ppm. The retention time window was 0.3 min, with the intensity scaling factors of 2-10. In addition, extracted ion chromatographic analysis (EIC) was applied to process the LC-MS datasets of the ADC incubations samples to find known or predicted payload-containing catabolites. Furthermore, acquired LC-MS/MS datasets of the ADC incubation samples were processed using product ion filter (PIF) to search for payload-containing catabolites that generated targeted product ions under CID. For example, the major payload-containing catabolites of T-DM1 (Lys-MCC-DM1) generated a major fragment at m/z 547.2207 so that PIF of m/z 547.2207 was used to process the LC-MS/MS dataset of the incubation sample of T-DM1 to find its payload-containing catabolites that generated the same fragment ion.

Results

Detection and structural characterization of payload-containing catabolites of T-DM1 in liver lysosomal incubation

Results from analyzing the T-DM1 incubation sample (48 h) in human liver lysosomes by LC-UV/HRMS are displayed in Fig. 1. The LC-UV (Fig. 1A) and unprocessed LC-HRMS (Fig. 1B) profile of the sample revealed a pair of major PCCs, L7 and L8 (Lys-MCC-DM1) of T-DM1. PATBS-processed LC-MS profile (Fig. 1C) showed a pair of the major payload-related catabolites, L7 and L8 (Lys-MCC-DM1, and a pair of minor isomers L9 and L10 (Tyr-MCC-DM1). The product ion spectra and proposed structures of L7 and L9 are displayed in Fig. 2A and 2B. In addition, the raw LC-MS/MS dataset of the incubation sample was processed using PIF of m/z 547.22 that is a major product ion of L7 and L9 (Fig. 2A and 2B). As displayed in the PIF-processed ion chromatogram (Fig. 1D), several PCCs (L1-L6, L11) were detected in addition to L7-L10. An extracted ion chromatogram of all detected payload-containing components is displayed in Fig. 1E. Product ion spectra and proposed structures of L5 and L1 as well as L3 and L11 are presented in Fig. 2 and Fig. S1, respectively. A summary of all detected and identified T-DM1 catabolites formed in the incubations with human liver lysosomes are presented in Table 1. The major (L7 and L8) and minor (L11 and L12) PCCs of T-DM1 were previously observed in rats after dosing radiolabeled T-DM1 (Saad et al., 2015). The rest of the T-DM1 catabolites were first observed in this study based on our best knowledge.

Detection and structural characterization of payload-containing catabolites of ADC-1 in liver S9 incubations

ADC-1 was incubated with rat, monkey, and human liver S9 followed by detecting and characterizing released PCCs using the LC-HRMS approach. Unprocessed ion chromatograms of the ADC-1 incubation sample in monkey liver S9 for 48 h (Fig. 3A) did not display any payload-related components due to their low concentrations and the presence of large amounts of endogenous components and peptides generated from ADC antibody hydrolysis. The background subtraction processing using the LC-MS data of the antibody incubation sample as a control was able to remove most endogenous components and peptides without payload to display a major payload-containing catabolite, M4 (Fig. 3C). The second step of background subtraction processing using the LC-MS data of the pre-incubation sample of ADC-1 in monkey S9 completely removed unrelated components to display three additional minor PCCs of ADC-1, M1, M2 and M3 (Fig. 3D). Product ion spectra and proposed structures of M1-M4 are presented in Fig. 4 and Fig. S2. The detected and identified PCCs of ADC-1 in incubations with rat,

monkey, and human liver S9 for 48 h are summarized in Table 2. The PIF processing using fragment ions of M4 (Fig. 4D) detected M4, but did not find any other catabolites of ADC-1 since product ion spectral data of M1, M2 and M4 were not acquired in the DDA acquisition.

Detection and structural characterization of payload-related components of ADC-1 in tumor cells

ADC-1 and its control antibody were further incubated in breast cancer cells for 48 hours to investigate metabolism of ADC-1 in targeted cancer cells. The total ion chromatogram of the ADC-1 incubation sample did not show any payload-containing catabolites of ADC-1 (Fig. 5A). PATBS-processed ion chromatogram (Fig. 5B) confirmed that M4 was a single payload-containing component released from ADC-1 in the incubation with the breast cancer cells. The use of targeted EIC or PIF did not detect any payload-containing catabolites of ADC-1 except for M4 in the cancer cell incubation.

Discussions

In this study, a novel LC-HRMS method was developed and applied for detection and identification of PCCs of non-cleavable ADCs, which were formed in ADC incubations with liver lysosomes and S9 as well as cancer cells. The LC-HRMS method employed intensity-dependent acquisition to collect accurate full scan MS and MS/MS datasets of *in vitro* incubation samples. To search for PCCs of the testing ADC, recorded LC-MS datasets of a testing ADC and control incubation samples were processed using PATBS, an untargeted data mining tool, which has been effectively used for detecting drug metabolites or xenobiotic components in a test sample that are absent or have much lower concentration in a control sample (Xing et al., 2015; Zhu et al., 2009). In parallel, targeted PIF was employed to process LC-MS/MS datasets to find payload-containing components that generated one or a few known or predictable product ion under CID. In addition, EIC was used to confirm detected PCCs by PATBS and PIF and to search for any predictable catabolites of a testing ADC and their metabolites formed in incubations. After payload-containing components in an incubation sample were detected, via the data mining, their MS/MS spectral data were retrieved from the acquired LC-MS/MS dataset. Structures of the detected PCCs were characterized based on their spectral interpretation. If MS/MS spectrum of a PCC was not triggered in the acquisition, additional LC-HRMS analyses of the same sample using targeted product ion scanning were carried out to acquire its product ion spectrum.

PATBS has been extensively used in finding unknown metabolites of small molecular drug *in vitro* and *in vivo* (Zhang and Yang, 2008; Zhang et al., 2008; Wu et al., 2016; Chen et al., 2016). In this study, the effectiveness of PATBS in untargeted detection of PCCs of non-cleavable ADCs was first evaluated by identifying released payload-containing components in an incubation sample of T-DM1 with human liver lysosomes. It is reported that the uncleavable ADC mainly releases payload derivatives L7 and L8 (a pair of Lys-MCC-DM1) via protein hydrolysis in rats (Shen et al., 2012) and cancer cells (Erickson et al., 2012; Baron et al., 2015). As shown in the LC-UV and unprocessed LC-MS profiles (Fig. 1A and 1B), T-DM1 released two major payload-containing components, L7 and L8, in the liver lysosomal incubation (Fig. 2A), consistent with the reported data. The background subtraction processing was able to

remove most background noises and ADC peptides without payload and revealed two additional minor PCCs, L9 and L10 (Tyr-MCC-DM1) (Fig. 2B and Table 1). The results confirm the usefulness of the untargeted data mining tool in finding PCCs of a non-cleavable ADC in vitro.

Background subtraction was further applied to identification of payload-containing catabolites of ADC-1 in incubations with rat, monkey, and human liver S9 (Fig. 3). The unprocessed LC-MS profile of the test ADC incubation sample in monkey liver S9 (Fig. 3A) did not display any payload-related components. After background subtraction by the control antibody incubation sample, the processed LC-MS profile showed the major payload-containing compound, M4, which was generated from a cysteine binding site of the payload in the ADC-1 antibody (Fig. 3C). The sequential background subtraction using a pre-incubation sample of ADC-1 generated a better result (Fig. 3D), in which not only three additional minor payload-containing components M1, M2 and M3 were revealed (Table 1), but also there were no significant false positive peaks. In addition to the effective detection of unknown catabolites of non-cleavable ADCs, PATBS can simplify full scan MS spectral data of the detected catabolites for identification of their protonated molecules in single or double charges (Tables 1 and 2). For example, the unprocessed full scan MS spectrum of catabolite M1 of ADC-1 displayed the doubly charged molecule at m/z 587.8429 along with several major interference ions (Fig. 4A). In contrast, the background subtracted full scan MS spectrum of catabolite M1 displayed only the analyte ion at m/z 587.8429 with minimal other ions from coeluted components irrelevant to M1 (Fig. 4B).

The catabolism of ADC in lysosomes is the breakdown of the antibody protein into a huge number of smaller peptides and ultimately into amino acids. Usually, an ADC molecule contains several payloads so that over 99% of smaller peptides generated from the ADC catabolism don't contain the payload moiety. Most likely, the same peptides can be generated via the catabolism of the same antibody (without payload and linker). The working mechanism of the PATBS software is to find analyte ions of interests that are displayed in individual accurate full scan MS spectra of the testing sample LC-MS dataset but are not present or have significantly lower levels in the same MS spectral data of a control sample regardless of their molecular weights, mass defects, and fragmentations (Zhang et al., 2008). Therefore, the key element of the effective application of PATBS to finding PCCs of a testing ADC is the use of

suitable control sample(s). In this study, the same antibody of a testing ADC (without the payload and linker) was used as a control sample of the background subtraction processing. Consequently, peptides without payload from protein hydrolysis of the ADC were effectively removed by background subtraction (Fig. 1C and 3C). Furthermore, the application of a sequential background subtraction using an ADC-1 pre-incubation sample (0 h) further removed interference components from the ADC dosing solution, generating a very clear and complete profile of PCCs of ADC-1 (Fig. 3D).

As a complementary data mining tool, PIF has been used to search for drug metabolites that generated a specific product ion in an acquired LC-MS/MS dataset (Tian et al., 2015; Zhang et al., 2017; Zhu et al., 2011). In this study, we found the major payload-containing catabolites L7 and L8 of T-DM1 generated a very significant product ion at m/z 547.22 under CID (Fig. 2A). Then the product ion filtering of m/z 547.22 was applied to searching for any PCCs that generated the same product ion in the LC-MS/MS dataset. As a result, eight minor payload-containing catabolites of T-DM1 were revealed in the PIF processed chromatogram (Fig. 1D, Table 1). The example indicates that targeted PIF data processing was more sensitive than untargeted background subtraction and can be used without any control sample. However, the detection of a payload-containing catabolite by PIF must meet specific conditions: the product ion spectrum of an analyte must be automatically acquired and contain the targeted product ion. For example, product ion spectra of all detected payload-containing catabolites of T-DM1 by PIF have the ion at m/z 547.2207 (Fig. 2, Fig. S1). EIC that searches for known or predictable ion species in LC-MS dataset is another targeted data mining tool used in this study. However, as shown in Table 1, the detected payload-containing catabolites had various types of structures, such as payloads with one, two or three different amino acid(s), which would be very difficult to predicted. An additional application of EIC in this study is to confirm payload derivatives detected by PIF (Fig. 1E) since the EIC-processed chromatogram displayed true chromatographic peaks of payload-containing components, while a PIF-processed ion chromatogram usually displayed detected analyte components in a few lines rather than a chromatographic peak and some false positive signals (Fig. 1D).

In this study, the LC-HRMS-based intensity dependent acquisition method was used to analyze the T-DM1 incubation samples to trigger MS/MS spectral acquisition of 10 payload

derivatives (L1-L10) (Fig. 1D). The results not only enabled their detection by PIF of m/z 547.22, but also provided key information for structural characterization. In contrast, the DDA method did not trigger MS/MS acquisition of minor payload-containing catabolites (M1, M2 and M3) of ADC-1 when analyzing in the incubation samples of ADC-1 with liver S9 due to their low concentrations. Consequently, PIF cannot be applied for finding these PCCs. Recently, a background exclusion based DDA method was successfully applied to automated MS/MS acquisition of low levels of xenobiotics in biological samples (Zhu et al., 2020; Ruan and Comstock, 2021). The new DDA method may be very useful in data acquisition for profiling payload-containing catabolites of a non-cleavable ADC *in vitro*. As alternative methods, data independent acquisition methods such as “all ion fragmentation” (Bateman et al., 2009; Cho et al., 2012), SWATH) (Hopfgartner et al., 2012) and MS^E (Wrona et al., 2005; Bateman et al., 2007) may be useful for the task.

The LC-HRMS method developed in this study combined with *in vitro* systems such as acidified liver lysosomes and S9 and targeted cancer cell lines (Zhu et al., 2020; Erickson et al., 2012; Admo et al., 2017; Bessire et al., 2016; Liu et al., 2020) is a useful approach for rapid detection, structural characterization and quantitative estimation of payload-containing components generated from ADC catabolism *in vitro*. Results from such an *in vitro* experiment can be used to quickly evaluate the payload and/or linker design in early drug discovery. Ideally, an excellent non-cleavable ADC candidate should release a single major payload-containing catabolite with one or a few amino acids in liver lysosomal or S9 incubation. T-DM1 and ADC-1 are good examples as demonstrated in this study. Generation of multiple major PCCs from ADC catabolism could make the ADC preclinical evaluation and clinical development extremely difficult. Once a single major payload-containing component released *in vitro* from a cleavable or non-cleavable ADC is identified, the chemical standard of the major PCC should be prepared for drug interaction evaluation, such as CYP inhibition. In addition, *in vitro* major metabolic pathways of the PCC and associated metabolizing enzyme(s) should be determined since the inhibition of the metabolizing enzyme(s) by a co-administered drug could increase the exposure of the PCC in human, resulting significant drug interaction. Furthermore, the exposure of the major PPC of an ADC to animals and human should be quantitatively monitored in its safety and clinical studies using LC-MS and the chemical standard. Finally, the information of the *in vitro* release of the same major PCC from ADC catabolism in human and toxicological species is

critical in support of selecting toxicological species in the discovery safety evaluation. When an ADC drug candidate is in clinical development, the comparison of exposure levels of the PCC in human and toxicological species should be determined. Results from the study can assess if the toxicity of the PCC is fully evaluated in ADC safety testing in animals.

In summary, the study demonstrates the advantages of this LC-HRMS method. First, untargeted background subtraction processing of LC-MS dataset and use of the corresponding antibody as a control sample enabled selectively detecting payload-containing components of a non-cleavable ADC regardless of their molecular weights, charge states, fragmentations, and mass defect values. Second, the use of common product ion(s) from payload-containing derivatives to perform product ion filtering of LC-MS/MS data can detect PCCs with better analytical sensitivity if their product ion spectra are automatically acquired. Results from detection and structural characterization of payload-containing components generated from ADC catabolism in liver lysosomes and S9 fraction can provide valuable information for optimizing payload design, verifying toxicological species for ADC safety testing, and selecting the major payload-containing component(s) for evaluation of *in vitro* DDI potentials and exposures in animals and human. However, the effectiveness of this LC-HRMS method for profiling *in vivo* payload-containing catabolites of ADCs remains to be tested.

AUTHORSHIP CONTRIBUTIONS

Participated in research design: Zhu, Cai, Shi, Guo, Tao

Conducted experiments: Cai, Shi, Guo, Li, Cao

Contributed new reagents or analytic tools: Guo, Cao

Performed data analysis: Cai, Shi, Zhu, Li

Wrote or contributed to the writing of the manuscript: Cai, Shi, Zhu, Shen, Tao

REFERENCES

- Adamo M, Sun G, Qiu D, Valente J, Lan W, Song H and Krishnamurthy G (2017) Drug-to-antibody determination for an antibody-drug-conjugate utilizing cathepsin B digestion coupled with reversed-phase high-pressure liquid chromatography analysis. *Journal of Chromatography A* **1481**: 44-52.
- Anami Y, Yamazaki CM, Xiong W, Gui X, Zhang N, An Z and Tsuchikama K (2018) Glutamic acid–valine–citrulline linkers ensure stability and efficacy of antibody–drug conjugates in mice. *Nature Communications* **9(1)**: 2512.
- Bargh JD, Isidro-Llobet A, Parker JS and Spring DR (2019) Cleavable linkers in antibody–drug conjugates. *Chemical Society Reviews* **48(16)**: 4361-4374.
- Bargh JD, Walsh SJ, Ashman N, Isidro-Llobet A, Carroll JS and Spring DR (2021) A dual-enzyme cleavable linker for antibody–drug conjugates. *Chemical Communications* **57(28)**: 3457-3460.
- Baron JM, Boster BI and Barnett CM (2015) Ado-trastuzumab emtansine (T-DM1): a novel antibody-drug conjugate for the treatment of HER2-positive metastatic breast cancer. *Journal of oncology pharmacy practice: official publication of the International Society of Oncology Pharmacy Practitioners* **21(2)**: 132-142.
- Bateman KP, Castro-Perez J, Wrona M, Shockcor JP, Yu K, Oballa R and Nicoll-Griffith DA (2007) MSE with mass defect filtering for in vitro and in vivo metabolite identification. *Rapid communications in mass spectrometry* **21(9)**: 1485-1496.
- Bateman KP, Kellmann M, Muenster H, Papp R and Taylor L (2009) Quantitative-qualitative data acquisition using a benchtop Orbitrap mass spectrometer. *Journal of the American Society for Mass Spectrometry* **20(8)**: 1441-1450.
- Bessire AJ and Subramanyam C (2020) LC/MS Methods for Studying Lysosomal ADC Catabolism. *Methods in molecular biology (Clifton, N.J.)* **2078**: 341-351.

- Bessire AJ, Ballard TE, Charati M, Cohen J, Green M, Lam MH and Subramanyam C (2016) Determination of Antibody-Drug Conjugate Released Payload Species Using Directed in vitro Assays and Mass Spectrometric Interrogation. *Bioconjugate chemistry* **27(7)**: 1645-1654.
- Bolleddula J, Shah A, Shadid M, Kamali A, Smith MD and Chowdhury SK (2020) Pharmacokinetics and Catabolism of [(3)H]TAK-164, a Guanylyl Cyclase C Targeted Antibody-Drug Conjugate. *Drug metabolism and disposition: the biological fate of chemicals* **48(11)**: 1239-1245.
- Chau CH, Steeg PS and Figg WD (2019) Antibody-drug conjugates for cancer. *Lancet (London, England)* **394(10200)**: 793-804.
- Chen C, Wohlfarth A, Xu H, Su D, Wang X, Jiang H and Zhu M (2016) Untargeted screening of unknown xenobiotics and potential toxins in plasma of poisoned patients using high-resolution mass spectrometry: Generation of xenobiotic fingerprint using background subtraction. *Analytica chimica acta* **944**: 37-43.
- Cho R, Huang Y, Schwartz JC, Chen Y, Carlson TJ and Ma J (2012) MS(M), an efficient workflow for metabolite identification using hybrid linear ion trap Orbitrap mass spectrometer. *Journal of the American Society for Mass Spectrometry* **23(5)**: 880-888.
- Erickson HK, Lewis Phillips GD, Leipold DD, Provenzano CA, Mai E, Johnson HA and Tibbitts J (2012) The effect of different linkers on target cell catabolism and pharmacokinetics/pharmacodynamics of trastuzumab maytansinoid conjugates. *Molecular cancer therapeutics* **11(5)**: 1133-1142.
- García-Alonso S, Ocaña A and Pandiella A (2018) Resistance to Antibody-Drug Conjugates. *Cancer research* **78(9)**: 2159-2165.
- Han TH and Zhao B (2014) Absorption, distribution, metabolism, and excretion considerations for the development of antibody-drug conjugates. *Drug metabolism and disposition: the biological fate of chemicals* **42(11)**: 1914-1920.
- Hinrichs MJ and Dixit R (2015) Antibody Drug Conjugates: Nonclinical Safety Considerations. *The AAPS journal* **17(5)**: 1055-1064.
- Hopfgartner G, Tonoli D and Varesio E (2012) High-resolution mass spectrometry for integrated qualitative and quantitative analysis of pharmaceuticals in biological matrices. *Analytical and bioanalytical chemistry* **402(8)**: 2587-2596.

- Khera E and Thurber GM (2018) Pharmacokinetic and Immunological Considerations for Expanding the Therapeutic Window of Next-Generation Antibody-Drug Conjugates. *BioDrugs: clinical immunotherapeutics, biopharmaceuticals and gene therapy* **32(5)**: 465-480.
- Khongorzul P, Ling CJ, Khan FU, Ihsan AU and Zhang J (2020) Antibody-Drug Conjugates: A Comprehensive Review. *Mol Cancer Res* **18(1)**: 3-19.
- Kommineni N, Pandi P, Chella N, Domb AJ and Khan W (2020) Antibody drug conjugates: Development, characterization, and regulatory considerations. **31(6)**: 1177-1193.
- Kraynov E, Kamath AV, Walles M, Tarcsa E, Deslandes A, Iyer RA and Moore DJ (2016) Current Approaches for Absorption, Distribution, Metabolism, and Excretion Characterization of Antibody-Drug Conjugates: An Industry White Paper. *Drug metabolism and disposition: the biological fate of chemicals* **44(5)**: 617-623.
- Liu H, Bolleddula J, Nichols A, Tang L, Zhao Z and Prakash C (2020) Metabolism of bioconjugate therapeutics: why, when, and how? *Drug metabolism reviews* **52(1)**: 66-124.
- Mukherjee A, Waters AK, Babic I, Nurmemmedov E, Glassy MC, Kesari S and Yenugonda VM (2019) Antibody drug conjugates: Progress, pitfalls, and promises. *Human antibodies* **27(1)**: 53-62.
- Nobre CF, Newman MJ, DeLisa A and Newman P (2019) Moxetumomab pasudotox-tdfk for relapsed/refractory hairy cell leukemia: a review of clinical considerations. *Cancer Chemotherapy and Pharmacology* **84(2)**: 255-263.
- Pander G, Uhl P, Kühl N, Haberkorn U, Anderl J and Mier W (2022) Antibody–drug conjugates: What drives their progress? *Drug Discovery Today*.
- Peters C and Brown S (2015) Antibody-drug conjugates as novel anti-cancer chemotherapeutics. *Bioscience reports* **35(4)**.
- Rangan VS, Myler H, Kozhich A, Wang J, Randazzo R and Deshpande S (2015) Biotransformation and stability of antibody-drug conjugates: payload metabolism and linker cleavage delineation. *Bioanalysis* **7(11)**: 1319-1323.
- Ruan Q and Comstock K (2021) A New Workflow for Drug Metabolite Profiling by Utilizing Advanced Tribid Mass Spectrometry and Data-Processing Techniques. *Journal of the American Society for Mass Spectrometry* **32(8)**: 2050-2061.

- Saad OM, Shen BQ, Xu K, Khojasteh SC, Girish S and Kaur S (2015) Bioanalytical approaches for characterizing catabolism of antibody-drug conjugates. *Bioanalysis* **7(13)**: 1583-1604.
- Shadid M, Bowlin S and Bolleddula J (2017) Catabolism of antibody drug conjugates and characterization methods. *Bioorganic & medicinal chemistry* **25(12)**: 2933-2945.
- Shen BQ, Bumbaca D, Saad O, Yue Q, Pastuskovas CV, Khojasteh SC and Girish S (2012) Catabolic fate and pharmacokinetic characterization of trastuzumab emtansine (T-DM1): an emphasis on preclinical and clinical catabolism. *Current drug metabolism* **13(7)**: 901-910.
- Su D and Zhang D (2021) Linker Design Impacts Antibody-Drug Conjugate Pharmacokinetics and Efficacy via Modulating the Stability and Payload Release Efficiency. *Frontiers in pharmacology* **12**: 687926.
- Tian T, Jin Y, Ma Y, Xie W, Xu H, Zhang K and Du Y (2015) Identification of metabolites of oridonin in rats with a single run on UPLC-Triple-TOF-MS/MS system based on multiple mass defect filter data acquisition and multiple data processing techniques. *Journal of chromatography. B, Analytical technologies in the biomedical and life sciences* **1006**: 80-92.
- Wei C, Su D, Wang J, Jian W and Zhang D CPR (2017) LC–MS Challenges in Characterizing and Quantifying Monoclonal Antibodies (mAb) and Antibody-Drug Conjugates (ADC) in Biological Samples. *Current Pharma. Reports* **4**: 45-63.
- Widdison W, Wilhelm S, Veale K, Costoplus J, Jones G, Audette C and Chari R (2015) Metabolites of antibody-maytansinoid conjugates: characteristics and in vitro potencies. *Molecular pharmaceutics* **12(6)**: 1762-1773.
- Wrona M, Mauriala T, Bateman KP, Mortishire-Smith RJ and O'Connor D (2005) 'All-in-one' analysis for metabolite identification using liquid chromatography/hybrid quadrupole time-of-flight mass spectrometry with collision energy switching. *Rapid communications in mass spectrometry* **19(18)**: 2597-2602.
- Wu C, Zhang H, Wang C, Qin H, Zhu M and Zhang J (2016) An Integrated Approach for Studying Exposure, Metabolism, and Disposition of Multiple Component Herbal Medicines Using High-Resolution Mass Spectrometry and Multiple Data Processing

- Tools. *Drug metabolism and disposition: the biological fate of chemicals* **44(6)**: 800-808.
- Xing J, Zang M, Zhang H and Zhu M (2015) The application of high-resolution mass spectrometry-based data-mining tools in tandem to metabolite profiling of a triple drug combination in humans. *Analytica chimica acta* **897**: 34-44.
- Zhang D, Yu SF, Khojasteh SC, Ma Y, Pillow TH, Sadowsky JD and Hop C (2018) Intratumoral Payload Concentration Correlates with the Activity of Antibody-Drug Conjugates. *Molecular cancer therapeutics* **17(3)**: 677-685.
- Zhang H and Yang Y (2008) An algorithm for thorough background subtraction from high-resolution LC/MS data: application for detection of glutathione-trapped reactive metabolites. *Journal of mass spectrometry* **43(9)**: 1181-1190.
- Zhang H, Ma L, He K and Zhu M (2008) An algorithm for thorough background subtraction from high-resolution LC/MS data: application to the detection of troglitazone metabolites in rat plasma, bile, and urine. *Journal of mass spectrometry* **43(9)**: 1191-1200.
- Zhang X, Yin J, Liang C, Sun Y and Zhang L (2017) UHPLC-Q-TOF-MS/MS Method Based on Four-Step Strategy for Metabolism Study of Fisetin in Vitro and in Vivo. *Journal of agricultural and food chemistry* **65(50)**: 10959-10972.
- Zhu C, Cai T, Jin Y, Chen J, Liu G, Xu N and Zhu M (2020) Artificial intelligence and network pharmacology based investigation of pharmacological mechanism and substance basis of Xiaokewan in treating diabetes. *Pharmacological research* **159**: 104935.
- Zhu P, Ding W, Tong W, Ghosal A, Alton K and Chowdhury S (2009) A retention-time-shift-tolerant background subtraction and noise reduction algorithm (BgS-NoRA) for extraction of drug metabolites in liquid chromatography/mass spectrometry data from biological matrices. *Rapid communications in mass spectrometry: RCM* **23(11)**: 1563-1572.
- Zhu X, Huo S, Xue C, An B and Qu J (2020) Current LC-MS-based strategies for characterization and quantification of antibody-drug conjugates. *Journal of pharmaceutical analysis* **10(3)**: 209-220.
- Zhu X, Kalyanaraman N and Subramanian R (2011) Enhanced screening of glutathione-trapped reactive metabolites by in-source collision-induced dissociation and extraction of

product ion using UHPLC-high resolution mass spectrometry. *Anal. Chem.* **83**(24): 9516-9523.

FOOTNOTES

Finding:

This study was funded by WuXi AppTec.

Financial Disclosure Statement:

No author has an actual or perceived conflict of interest with the contents of this article.

FIGURE LEGENDS

Figure. 1. Analysis of a liver lysosomal incubation sample of T-DM1 by LC-UV/HRMS. (A) LC/UV profile. (B) TIC of the full scan MS dataset. (C) Background subtraction-processed TIC of the full scan MS dataset. (D) PIF (m/z 547.2207)-processed TIC of full scan MS/MS dataset. (E) Extracted ion chromatogram of all detected metabolite. T-DM1 was incubated at a concentration of 0.5 mg/mL for 48h.

Figure. 2. Product ion spectra and proposed structures of payload-containing components released from T-DM1 in incubation with lysosomes. (A) L7. (B) L9. (C) L5. (D) L1.

Figure. 3. LC-HRMS detection of released payload-containing catabolites of ADC-1 in monkey liver S9 incubation for 48 h. (A) A base peak chromatogram of the ADC-1 incubation. (B) A base peak chromatogram of the control antibody incubation in monkey liver S9 for 48 h. (C) A base peak chromatogram of the ADC-1 incubation after background subtraction using the LC-HRMS data of the control antibody incubation. (D) A base peak chromatogram of the ADC-1 incubation after sequential background subtractions by LC-HRMS data sets of the control antibody and the ADC-1 incubation sample in 0 h.

Figure. 4. Mass spectral data of the ADC-1 incubation in monkey liver S9 for 48 h. Full scan MS spectrum at RT 26.39 min (M1) from the LC-MS dataset of the ADC-1 incubation without background subtraction (A) and with background subtraction (B). (C) MS² spectrum of M1. (D) MS² spectrum of M4.

Figure. 5. Detection and characterization of a released payload-containing component in incubation of ADC-1 in tumor cells for 48 h. (A) Total ion chromatogram of the raw LC-MS dataset. (B) Background subtraction processed total ion chromatogram.

Tables

Table 1. A summary of payload-containing components released in incubation of T-DM1 in human liver lysosomes for 48 h.

Metabolite	RT (min)	Observed mass (m/z)	ID	Theoretical mass (m/z)	Mass error (ppm)
L1	7.39	684.8181 (2+)	Lys-His-Lys-MCC-DM1	684.8191 (2+)	-1.5
L2	7.54	684.8184 (2+)	Lys-His-Lys-MCC-DM1	684.8191 (2+)	-1.0
L3	7.99	673.8077 (2+)	Arg-Ser-Lys-MCC-DM1	673.8088 (2+)	-1.6
L4	8.15	673.8091 (2+)	Arg-Ser-Lys-MCC-DM1	673.8088 (2+)	0.4
L5	8.14	671.2960 (2+)	His-Thr-Lys-MCC-DM1	671.2955 (2+)	0.7
L6	8.30	671.2954 (2+)	His-Thr-Lys-MCC-DM1	671.2955 (2+)	-0.1
L7	9.39	1103.4731	Lys-MCC-DM1	1103.4772	-3.7
L8	9.57	1103.4734	Lys-MCC-DM1	1103.4772	-3.4
L9	10.50	1138.4425	Tyr-MCC-DM1	1138.4456	-2.7
L10	10.62	1138.4429	Tyr-MCC-DM1	1138.4456	-2.4
L11	11.68	975.3793	MCC-DM1	975.3823	-3.1
L12	11.80	975.3788	MCC-DM1	975.3823	-3.6

Table 2. Detection and characterization of payload-containing components released from incubations of ADC-1 with rat, monkey and human liver S9 for 48 h.

Metabolite	RT (min)	Molecular formula	<i>m/z</i>	ID	Rat	Monkey	Human
M1	26.39	C ₅₈ H ₉₅ N ₉ O ₁₄ S ₂	587.8433 (+2) 1174.6792(+1)	Lys-cys-MMAF	0.19%	0.81%	1.11%
M2	27.62	C ₄₅ H ₇₆ N ₆ O ₉	423.2910 (+2) 845.5747 (+1)	Hydrolysis of M4	1.44%	2.16%	0.83%
M3	28.91	C ₅₆ H ₉₀ N ₈ O ₁₅ S	574.3196 (+2) 1147.6320 (+1)	Thr-cys-MMAF	0.10%	2.65%	0.98%
M4	29.09	C ₅₂ H ₈₃ N ₇ O ₁₃ S ₂	523.7958 (+2) 1046.5842 (+1)	Cys-MMAF	98.27%	94.38%	97.08%

Fig. 1.

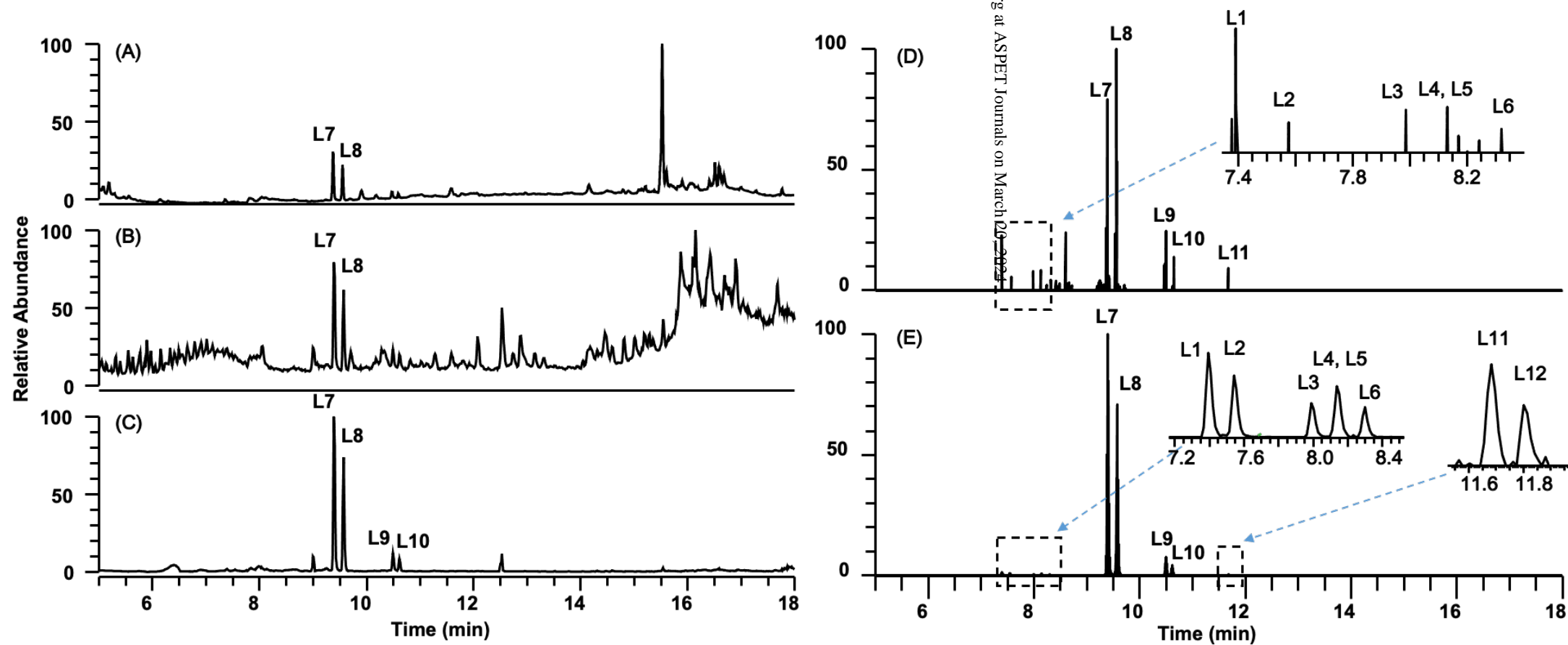


Fig. 2.

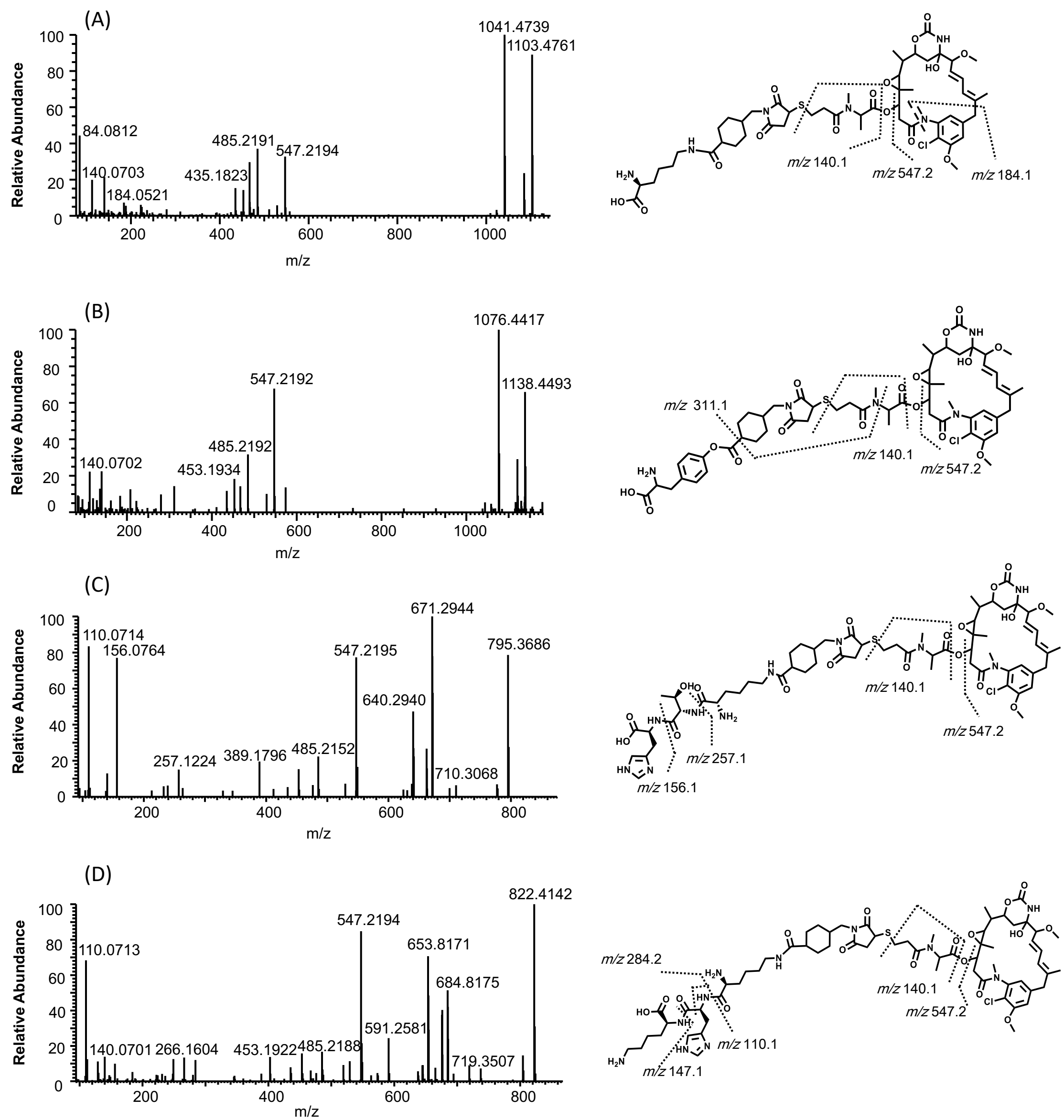


Fig. 3.

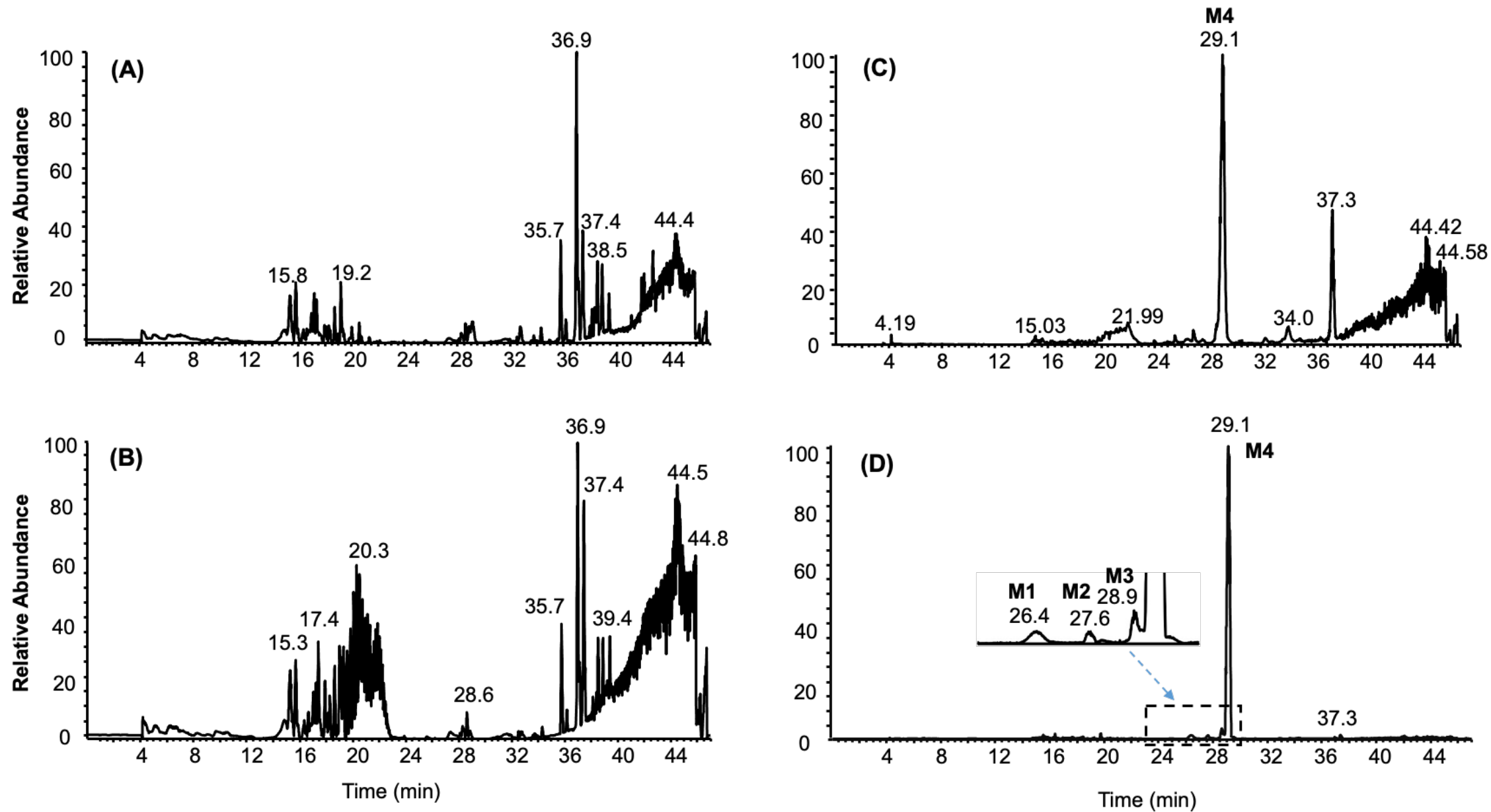
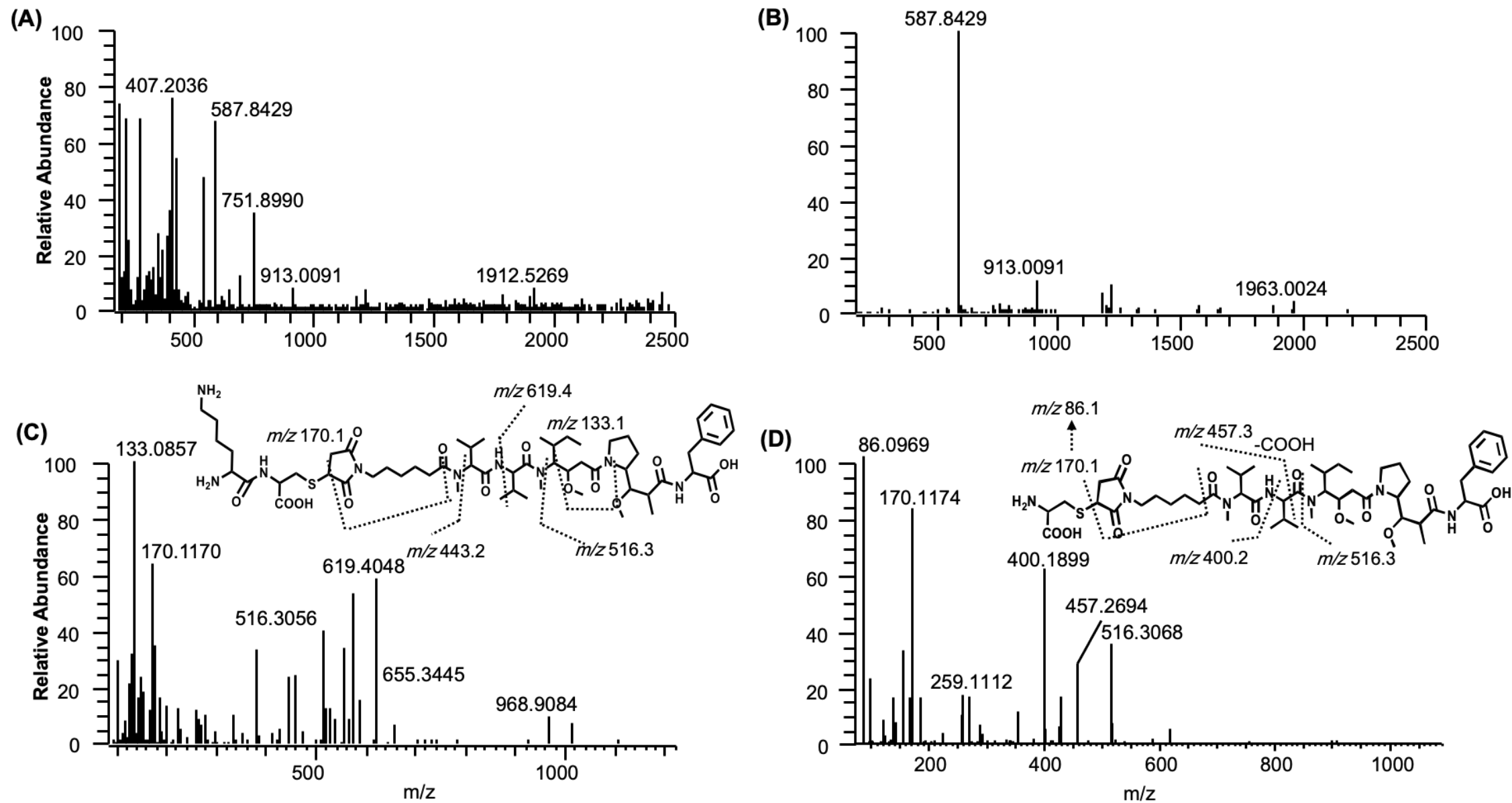



Fig. 4.





Mass spectrum (A) showing relative abundance versus m/z. The base peak is at m/z 50.1. Other labeled peaks are at m/z 13.2 and 15.2.

